ISSN: 0974-5823 Vol. 7 No. 1 January, 2022

*International Journal of Mechanical Engineering*

# Tube Spinning Using Functionally Graded Ballizing

M. H. Kassar[1], K. I. Ahmed[2], M. N. Elsheikh[3], and S. Z. El-Abden[1]

[1]Mechanical Engineering Department, Minia University, El Minia, Egypt.

[2]Mechanical Engineering Department, King Abdulaziz University, Jeddah 21589, KSA.

[1]Mechanical Engineering Department, Bani Sweef University, Bani Sweef, Egypt.

**ABSTRACT**

**The thin-walled cup is considered an important part of developing aeronautic, aerospace, rocket capsule components, military industry, and other manufacturing processes for daily use parts. These parts can be produced by conventional spinning with rollers or by ball spinning process. The recent development of ball spinning of tubes and thin wall thickness cups faces the challenge of limiting the large reductions due to built-up material formation in front of the forming balls. The current study introduces a new ball set design to overcome the pile-up problem during large reduction tube spinning.**

**The proposed design consists of 4 balls distributed in four planes, having one ball in each plane. The first plane is set to suppress the pile-up formation, the second, the third, and the fourth planes are set for the main forming process. Every two consecutive planes are shifted by 90 deg. from each other to contribute to the thickness reduction. The new design is investigated experimentally through Latine Hybercube Design of Experiments. The surface responses of the experimental results are statistically analyzed using second-order linear regression.**

**The results analysis shows that the new design has shown the potential to significantly overcome the pile-up formation in front of the forming balls at high thickness reduction operation. The optimum working conditions for minimum material pile-up, minimum average diameter deviation percentage, minimum average thickness deviation percentage, and minimum average surface roughness Ra are determined and presented.**

Keywords: Tube spinning, Conventional spinning, Ball spinning, pile-up, thin wall thickness cup.

## Introduction

Tube spinning is a forming process used to squeeze a thick-walled tube incrementally using forming rollers or balls to a thinner and longer tube. The process has the advantages of low tooling costs, low forming loads, tool flexibility, and near net shape production for various geometrical configurations [1]. Tube spinning using balls is more advantageous than conventional rollers for its smaller localized deformation zone and uniform distribution load. These characteristics of ball spinning ensure smaller forming loads and more accurate spun parts [2]. The material build-up in the front of the forming roller or ball is a communal limitation in tube spinning using either rollers or balls [3-4]. Many investigations had addressed these processes and their limitations due to material build-up.

Kalpakjian and Rajagopal [3] have concluded that the higher the tube thickness reduction, the roller feed rate, and the roller angle, the higher the material build-up in tube spinning using rollers. On the other hand, the higher the roller nose angle or tilt angle, the lower the material build-up. The two types of spinning, forward or backward, do not affect the build-up phenomena under the same conditions. In order to reduce the material build-up, the process parameters need to be controlled. A suggested method to reduce the build-up is using a flat roller with a cylindrical face tangential to the tube unspun part. Furthermore, the built-up defect is controlled in tube spinning using rollers by either multi-rollers or built-up suppresser roller shapes.

Kim et al. (2013) [5] investigated tube spinning using one roller by upper bound theory to find the optimum roller attack angle that generates the minimum axial forming loads. They concluded that the build-up phenomenon is mainly affected by the roller axial force, which increases the bulge in the front of the roller. They proved their claims by using a finite element simulation model.

Recent attempts [6-9] on tube spinning using rollers focused on obtaining analytical, statistical, or numerical models that correlate well with the experimental results. These studies are mainly about forming loads and controlling parameters such as roller feed, reduction percentage, attack angle, and roller nose radius. Bhatt and Raval [6-7] reported that lower feed and higher speed

produce more bulges under the forming roller. Wang et al. [9] concluded that the high flexibility of tubes with ultra-thin walls causes forming instability and material flow disorder. They recommended some optimum working conditions to overcome these instabilities.

Shuyong and Zhengyi (2008) [2] studied tube spinning using balls to investigate the effect of feed ratio and the ball diameter on the spinning force components. Their theoretical and experimental results showed that the deformation mechanics in backward ball spinning contributes to enhancing the plasticity of the tube material. In contrast, the deformation mechanics in forward ball spinning contributes to advancing the axial flow of the tube material. They also found that the tangential spinning force component significantly influences the formability of the spun parts. The study neither recommended an optimum feed ratio nor an optimum ball's diameter for producing minimum spinning force components for sound spun tubes.

Zhang et al. (2007) [10] studied ball spin forming to investigate the primary defect in the inner grooved copper tube's inner surface during ball spin forming. They proposed a finite element analysis showing that folding defects are formed on both sides, on one side of the fin and the bottom of the copper tubes' inner grooves. They concluded that the folding defects might be eliminated by reducing the difference between the blank tube's inner diameter and the plug's outer diameter. The simulated results suggested that the gap between the copper tube's inner surface and the plug directly led to the folding at the rounded corner between the partial fins and the fin bottom.

Jiang et al. (2008) [11] investigated manufacturing thin-walled tubular parts with longitudinal inner ribs using ball spinning. They studied the influence of ball diameter, feed ratio, wall thickness reduction, and the tubular blank's original wall thickness on the inner ribs' formability. They found that the formed inner ribs' height increases with the ball diameter, the wall thickness reduction ratio, and the feed ratio.

Jiang et al. (2009) [12] studied, experimentally, the effects of the spinning ball size on the final quality of the splined tooth and the metal flow under the ball. The results have shown that increasing the ball size improved the formability of the inner ribs and the tube wall material's steady flow under the forming balls. On the other hand, large ball size leads to low dimensional accuracy and inferior surface quality of the spun part. The study did not recommend optimum ball size or arrangement to compromise the splined tooth and outer surface quality.

Ahmed (2011) [13] introduced a numerical simulation of a new ball arrangement design for ball spinning of a splined tube. The balls are set at four different planes with progressive depth to simultaneously reduce mandrel tooth failure and overcome the material build-up. Although the simulation results proved the proposed design concept, it was not tested experimentally.

Li et al. (2011) [14] numerically investigated the ball spinning of thin-walled tubes made of super-alloy. The build-up phenomenon and its influencing factors like principal axis speed, axial feed rate, and wall thickness reduction were investigated using the finite element method (FEM). The experiment of the ball spinning process was performed based on the proper technical parameters obtained through simulation. The results showed that the build-up surface defect increases with the axial feed and wall thickness reduction. The study neither broaches how to overcome build-up nor defines optimum axial feed and optimum wall thickness reduction.

Jiang et al. (2013) [15] introduced ball spinning of nickel−titanium shape memory alloy (NiTi SMA) tubes at elevated temperatures. Based on the stress and strain fields, they showed that the NiTi SMA tube's outer wall is easier to meet the plastic yield criterion than the inner wall. The plastic deformation zone is caused to be in a three-dimensional compressive stress state. The finite element simulation result revealed a temperature rise of about 160 °C in the principal deformation zone of the NiTi alloy tube. Also, there is a temperature increase of about 300 °C on the ball at the contact area with the spun part.

Kuss et al. (2016) [16] proposed a 2D FEM model to predict the damage during ball spinning through statistical Design Of Experiments (DOE). Their results showed the need to increase the axial feed rate for a damage minimized process design. It has been shown that the increase in the tube wall reduction ratio or the feed rate increases the damage possibilities of ball spinning. These results were presented through 2D FEM simulation without experimental verification.

Chunjiang et al. (2017) [17] discussed the relationships between spinning depth, ball diameter, spinning feed, and ball-spinning force. They compared the results of a proposed analytical model, and that obtained by the finite element method shows a good correlation. They claimed that at spinning depth $h < d/2$, the ball-spinning pressure increases with the spin depth. However, at $h > d/2$, spinning pressure increases with the ball diameter and feed rate. These claims have neither been proven experimentally nor physically.

Abd-Eltwab et al. (2017) [18] investigated, experimentally, the ball spinning of a thin tube with inner ribs employing four balls in the same plane and same depth. They defined the ball set's optimum rotational speed and feed rate for obtaining sound splined tubes with no defects. However, they did not optimize the ball set for minimizing the material pile-up. Furthermore, they concluded that the increase in the material pile-up increased the deviation of their analytical model results from the experimental measurements.

Jiang et al. (2017) [19] studied ball spinning of a composite tube of copper and aluminum. They investigated the interface compatibility of the composite tubes during ball spinning through the finite element method and experiments. They concluded that finite element simulation results indicated that the two composite tubes are similar in distributing the stress and the strain in the deformation zone. Their study has neither presented proper working conditions nor optimum parametric relations.

Chunjiang et al. (2018) [20] provided a theoretical basis for further studying the tube deformation's accuracy and control method caused by the ball and the die deformations in the ball spinning process. They proposed a quasi-dynamic model using a bee colony intelligent algorithm to obtain the force at each point of the ball and its three-dimensional self-rotation speed under the given process parameters. Although claiming agreement with experimental, they have not presented any parametric study on the effect of process parameters on the calculated forces or motion.

Zhao et al. (2018) [21] investigated the effect of ball size, feed rate, and thickness reduction and their coupling on the tube spinning using nine balls. They obtained the optimum conditions through a statistical fitting of stress triaxiality obtained by finite element model results followed by experimental verification. They concluded that a larger feed ratio and smaller ball diameter improved the stress state in the deformation-affected zone. On the other hand, they reported increasing the ball diameter and reducing the feed ratio to improve the tube's plastic-forming capacity.

Zhao et al. (2019) [22] proposed a numerical model for calculating three-directional forces generated in ball spinning based on space analytic geometry theory. They compared their results to experimental results and reported that the calculation errors are significantly influenced by sliding friction and material pile-up.

Flow-forming of thin tubes has many parameters dependently controlling the final produced tube quality. Many researchers [23-29] have used Design Of Experiment (DOE) procedures to emphasize the significant contribution of each controlling parameter with an adequate number of experiments and simulations.

Davidson et al. (2008) [23] presented Taguchi L9 array to analyze three controlling working conditions of flow forming of Aluminum alloy 6061. They reported the optimum working conditions that produce maximum elongation without considering the surface quality or form accuracy.

Razani et al. (2011) [24] presented an L9 Taguchi array to find the effect of three working conditions on the flow forming of steel AISA 321. The reported optimum working conditions were based on the minimum out of roundness without considering the surface roughness of the produced tube.

Srinivasulu et al. (2013) [25] used the Box-Behnken design for their experiments to find the response surface due to three controlling working conditions of flow forming of Aluminum alloy 6082. They reported a second-order response surface for the surface roughness of the flow-formed tubes without considering other output qualities.

Abedini et al. (2015) [26] used Taguchi L9 array to find the effect of three working conditions on the flow forming of polyethylene pipes. Their study concerned the effect of the flow-forming working conditions on the mechanical properties of the produced pipes. The final quality and size of the produced pipes were not investigated.

De et al. (2021) [27] presented a full-factorial study on the effect of flow-forming working conditions on the produced surface roughness of Aluminum Alloy 6082. They concluded that the rollers' axial feed is the most significant with adverse effects on the produced surface roughness. It is worth noting that the effect of the relative positioning of the forming rollers is not considered in their study.

Wen et al. (2020) [28] investigated the effect of roller feed and thickness reduction on the formed wall bulge during the flow forming of long thin tubes. Although they have not used a known design of experiment procedures, they concluded that the thickness reduction is the most significant controlling factor for the wall bulge formation.

Khodadadi et al. (2020) [29] investigated experimentally and numerically, using DOE, the effect of four parameters on the final tooth height in the flow-forming of toothed tubes. Although they investigated just two-parameter levels, they reported a second-order relation between the investigated parameters and the final formed tooth height. They concluded that the reduction ratio is the most significant factor controlling tooth height.

The current paper introduces a new method of tube spinning using the multi-ball ballizing technique. The ballizing balls are adjusted with axial and radial shifts to overcome the metal build-up. The radial shift will be adjusted gradually using a grading function. Experimental investigations controlled by DOE and response surface correlation are used to emphasize the effect of the process parameters, and grading function on the final spun tube.

## Response Surface Theory

The response surface method is a statistical examination of the connections between explanatory factors and response variables. A second-order polynomial model is usually used to approximate and implement the factors' correlation to find an optimum answer using a series of well-planned trials. Using the appropriate design of experiments (DoE) has recently become popular for formulation optimization [30]. One of the most powerful design of experiments is Latin Hypercube Sampling design (LHS), which generates random points across the design space in equal-distances pattern [31]. The accuracy of the estimated surface response using LHS depends on the number of design points [32]. The procedure is as follow:

Suppose factors $x_i = x_1, x_2, \ldots, x_r$ and each factor range is $u_i = [a_i\ b_i]$, $i = 1,2,\ldots,r$.

To ensure all factors have all portions among its range, the range has been divided into ***n*** equiprobable intervals as $u_{i1}, \cup u_{i2}, \ldots, \cup u_{i2} = u_i,\ u_{ij} \cap u_{ik} = \emptyset$ and $P(x \in u_{ij}) = 1/n,$ where $j, k = 1,2,\ldots,n$

The cumulative probability for $j^{th}$ interval of $x_i$obtained as;

$$Prob_{ji} = \frac{(j-1)}{n} + \frac{r_{ij}}{n} \tag{1}$$

The probability can be transformed into the sample value $x_{ji}$ by the inverse of function $F(\cdot)$:

$$x_{ji} = F^{-1}\left(Prob_{ji}\right) \tag{2}$$

Hence the sample matrix is

$$x = \begin{bmatrix} x_{11} & x_{12} & \cdots & x_{1r} \\ x_{21} & x_{22} & \cdots & x_{2r} \\ \vdots & \vdots & \ddots & \vdots \\ x_{n1} & x_{n2} & \cdots & x_{nr} \end{bmatrix} \tag{3}$$

The ***n*** values of each factor are paired randomly with the ***n*** values of other factors, then the sample matrix of LHS will be [32]

$$x' = \begin{bmatrix} x'_{11} & x'_{12} & \cdots & x'_{1r} \\ x'_{21} & x'_{22} & \cdots & x'_{2r} \\ \vdots & \vdots & \ddots & \vdots \\ x'_{n1} & x'_{n2} & \cdots & x'_{nr} \end{bmatrix} \tag{4}$$

The number of design points of each method is generated to predict the second-order response surface coefficients. In fact, not all terms are significant, and some terms are left unused. The number of non-significant terms results in several degrees of freedom for the regression tool. The general form of the second-order polynomial with "n" variables and zero intercepts is represented in Eq. 7.

$$\hat{Q} = \sum_{i=1}^{n} a_i x_i + \sum_{i=1}^{n} \sum_{j=i}^{n} b_{ij} x_i\, x_j \tag{5}$$

Experimental Setup

A specially built test rig is installed on the carriage of a manually controlled universal lathe machine. The test rig, shown in Figure 1(a), consists of four forming balls made of hardened steel with a diameter of 21.0 mm welded to four adjustable housings on a four-jaw chuck. This four-jaw chuck is attached to the lathe carriage through a special frame, through which the flow-forming "axial feed" (***f***) is defined. The mandrel is made of hardened steel with a diameter of 60.0 mm and attached to the regular lathe chuck, controlling the rotational speed. The forming balls are adjustable at different heights from the mandrel stem, defining the "clearance" (***C***) parameter. The forming balls are installed in different axial planes with a fixed distance of 1.66 mm, which is the maximum possible distance to ensure roughness less than 30 um. The preformed cup is prepared by a conventional spinning process of Aluminum blanks (AL 1050) with an initial diameter of 100.0 mm and an initial thickness of 4.0 mm using a conical roller. The chemical compositions and mechanical properties of the Aluminum blanks are listed in Table 1 and Table 2. The blanks are annealed before performing conventional spinning, achieving the stress-strain behavior shown in Table 2. The preformed cups are also annealed after the conventional spinning process to relax the induced strain hardening.

**Table 1** Chemical composition of tested Aluminum blanks (AL1050).

| **Element** | **Al** | **Si** | **Fe** | **Cu** | **Mn** | **Mg** | **Zn** | **Cr** | **Ni** | **Ti** |
|---|---|---|---|---|---|---|---|---|---|---|
| **Percent** | 94.7 | 0.246 | 0.271 | 3.88 | 0.0388 | 0.0146 | 0.114 | 0.0266 | 0.1 | 0.0172 |
| **Element** | **Be** | **Ca** | **Pb** | **Sn** | **Sr** | **V** | **Bi** | **Zi** | **B** | **Ga** |
| **Percent** | 0.001 | 0.005 | 0.0288 | 0.243 | 0.001 | 0.0203 | 0.0997 | 0.183 | 0.004 | 0.0139 |
| **Element** | **Cd** | **Co** | **Ag** | **In** | | | | | | |
| **Percent** | 0.0417 | 0.0643 | 0.0137 | 0.0213 | | | | | | |

**Table 2** Measured plastic behavior of the tested material.

| | **Strength Coefficient** | **Strain Hardening Exponent** |
|---|---|---|
| **Before annealing** | K = 167 MPa | n=0.105 |
| **After annealing** | K = 123 MPa | n=0.149 |

Four working conditions are examined mainly; axial feed (***f***) mm/rev, mandrel rotating speed (***N***) rpm, clearance (***C***) for the first ball, and the gradient of the clearance for the rest three balls. For all test cases, the last ball is set at a fixed distance of 1.0 mm from the mandrel stem. The second and third balls are adjusted to form linear, convex, or concave decedent with the first and last balls, as illustrated in Figure 2. Linear descendent is achieved with gradient index (***m*** = 1.0), concave descendent is achieved with gradient index (m > 1.0), and convex descendent is achieved with gradient index (***m*** < 1.0), as shown in Figure 2. The clearance gradient through the four balls is functionally defined with a power grading function of power "***m***," shown in Eq. (6).

$$C_i = C_1 - \left(\frac{C_1 - 1}{3^m}\right)(i-1)^m \tag{6}$$

Where ***i*** is the ball number; 1, 2, 3, 4, and ***m*** is the grading index.

The combinations of these working conditions are examined through the Latine Hyber Cube uniform-space filling design-of-experiment method [32] using 36 cases, listed in Table 4. Each of the four examined parameters is tested at five levels, listed in Table 3. The column of the clearance of the last ball is grayed because it is constant throughout the course of the experiments. The columns of the clearances of the middle two balls are grayed columns as well because they are dependent on the clearance of the first ball and the grading index m.

The blanks with the tensile test specimens are cut using a laser cutting machine. The blanks are annealed before and after conventional spinning. Then the performed cups are tested with the ballizing testing setup based on the mentioned plan. Each experiment is repeated at least three times to ensure repeatability of the results. The thickness variations are measured using a dial gauge with an accuracy of 0.01 mm. The diameter variations are measured with digital vernier with an accuracy of 0.001. The blank and the cup weight are measured using a sensitive gold scale with an accuracy of 0.001 grams. Finally, the surface roughness is measured using profilometer Mitutoyo Talysurf SJ–310 model No (SURFTEST SJ-310).

**Table 3** Levels of the examined four parameters.

| | **1st Ball Clearance $C_1$ [mm]** | **Gradient Index-*m*** | **Feed *f* [mm/rev]** | **Mandrel Speed *N* [rpm]** |
|---|---|---|---|---|
| **Level 1** | 4.00 | 0.50 | 0.1 | 75 |
| **Level 2** | 4.25 | 0.80 | 0.2 | 150 |
| **Level 3** | 4.50 | 1.00 | 0.3 | 225 |
| **Level 4** | 4.75 | 1.25 | 0.4 | 300 |
| **Level 5** | 5.00 | 2.00 | 0.5 | 375 |

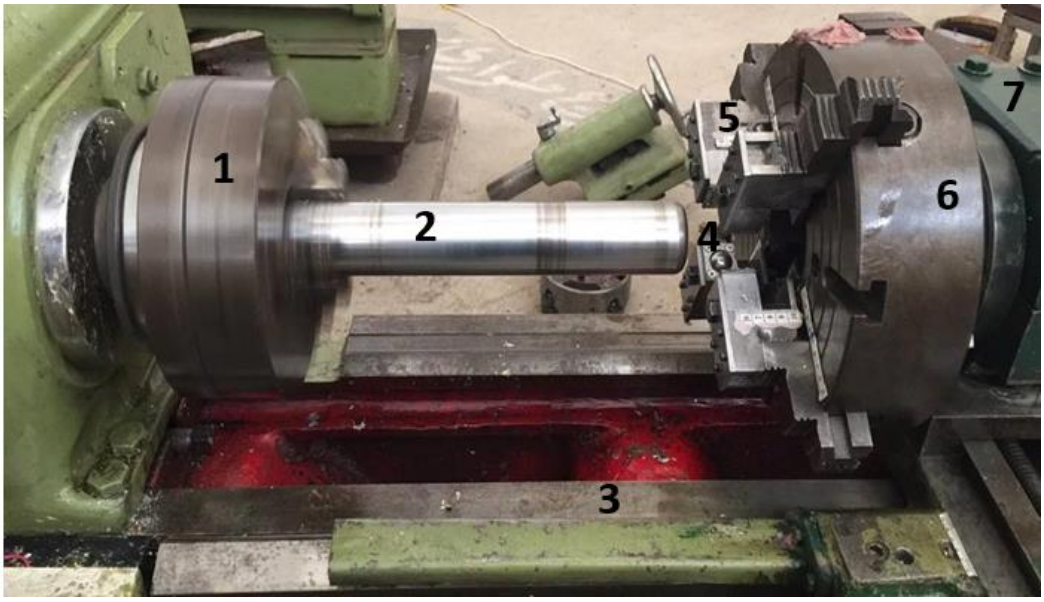


(a) Test rig components

(1) Lath Chuck, (2) Mandrel, (3) Lath bed, (4) Forming Balls, (5) Housing of balls, (6) Four Jew Chuck for forming tool, (7) Ballizing head holder.

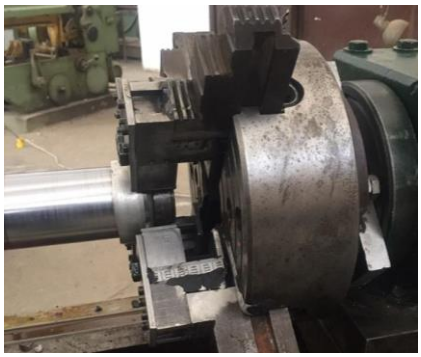

**(b)** Preformed cup before ballizing

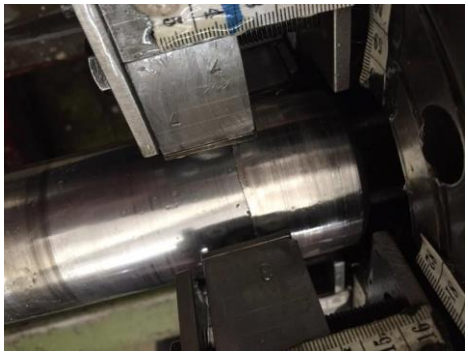

**(c)** Final cup after ballizing.

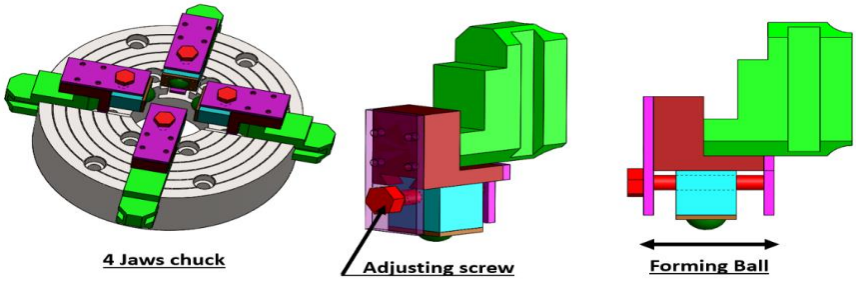


**(d)** Position adjusting mechanism.

**Figure 1** Ballizing test rig.

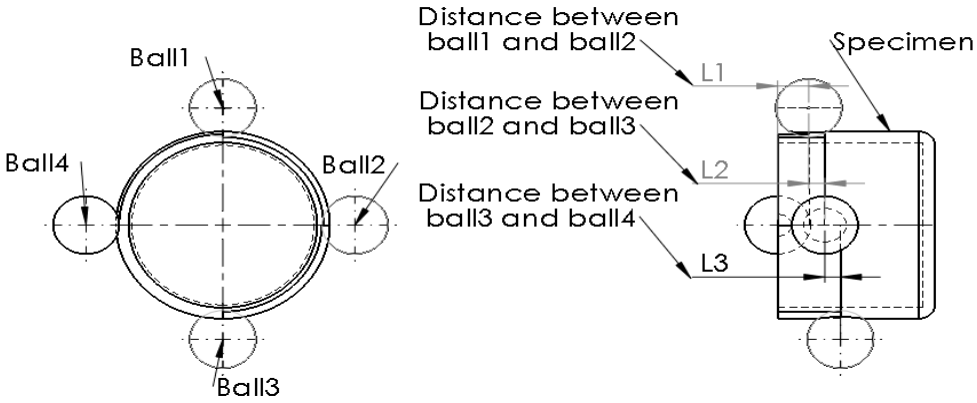


(a) Axial arrangement.

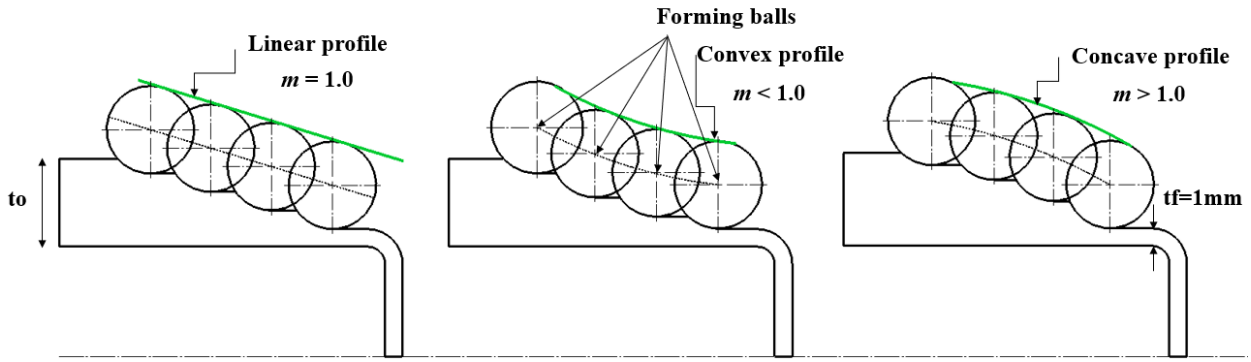


(b) Radial arrangement.

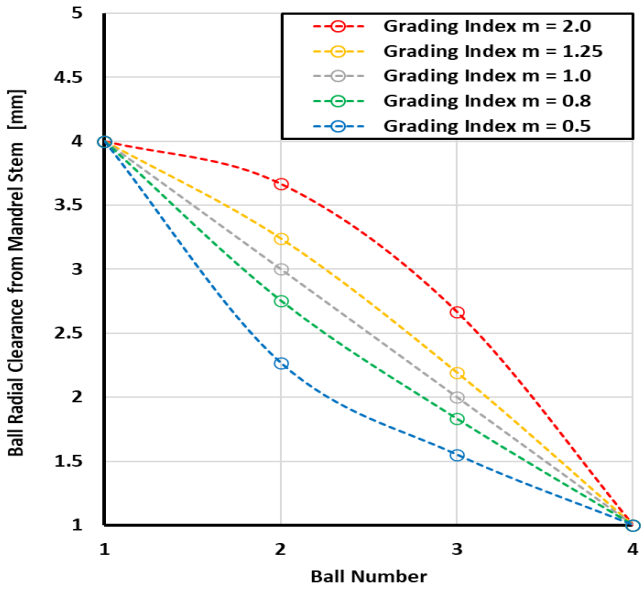


(c) The functionally graded tested profiles

**Figure 2:** Schematic of the four balls' gradient functions; linear (m=1.0), convex (m=0.5 and 0.8), and concave (m=1.25 and 2.0) profiles.

Table 4 Experiments plan and operating conditions.

| Test number | 1st Ball Clearance C1 [mm] | Gradient Index-m | 2nd Ball Clearance C2 [mm] | 3rd Ball Clearance C3 [mm] | 4th Ball Clearance C4 [mm] | Feed f [mm/rev] | Speed N [rpm] |
|---|---|---|---|---|---|---|---|
| 1 | 4 | 0.50 | 2.27 | 1.55 | 1 | 0.1 | 225 |
| 2 | 4 | 0.80 | 2.75 | 1.83 | 1 | 0.5 | 75 |
| 3 | 4 | 1.00 | 3.00 | 2.00 | 1 | 0.1 | 75 |
| 4 | 4 | 1.00 | 3.00 | 2.00 | 1 | 0.5 | 300 |
| 5 | 4 | 1.25 | 3.24 | 2.19 | 1 | 0.2 | 375 |
| 6 | 4 | 2.00 | 3.67 | 2.67 | 1 | 0.3 | 150 |
| 7 | 4 | 2.00 | 3.67 | 2.67 | 1 | 0.4 | 225 |
| 8 | 4.25 | 0.50 | 2.37 | 1.60 | 1 | 0.4 | 150 |
| 9 | 4.25 | 0.80 | 2.90 | 1.90 | 1 | 0.2 | 225 |
| 10 | 4.25 | 0.80 | 2.90 | 1.90 | 1 | 0.3 | 300 |
| 11 | 4.25 | 1.00 | 3.17 | 2.08 | 1 | 0.2 | 150 |
| 12 | 4.25 | 1.00 | 3.17 | 2.08 | 1 | 0.4 | 375 |
| 13 | 4.25 | 1.25 | 3.43 | 2.29 | 1 | 0.3 | 75 |
| 14 | 4.25 | 1.25 | 3.43 | 2.29 | 1 | 0.5 | 225 |
| 15 | 4.5 | 0.50 | 2.48 | 1.64 | 1 | 0.5 | 150 |
| 16 | 4.5 | 0.50 | 2.48 | 1.64 | 1 | 0.2 | 300 |
| 17 | 4.5 | 0.80 | 3.05 | 1.97 | 1 | 0.3 | 75 |
| 18 | 4.5 | 1.25 | 3.61 | 2.39 | 1 | 0.1 | 150 |
| 19 | 4.5 | 1.25 | 3.61 | 2.39 | 1 | 0.4 | 300 |
| 20 | 4.5 | 2.00 | 4.11 | 2.94 | 1 | 0.2 | 75 |
| 21 | 4.5 | 2.00 | 4.11 | 2.94 | 1 | 0.5 | 375 |
| 22 | 4.75 | 0.50 | 2.58 | 1.69 | 1 | 0.5 | 375 |
| 23 | 4.75 | 0.80 | 3.19 | 2.04 | 1 | 0.2 | 150 |
| 24 | 4.75 | 0.80 | 3.19 | 2.04 | 1 | 0.4 | 225 |
| 25 | 4.75 | 1.00 | 3.50 | 2.25 | 1 | 0.4 | 75 |
| 26 | 4.75 | 1.00 | 3.50 | 2.25 | 1 | 0.2 | 300 |
| 27 | 4.75 | 1.25 | 3.80 | 2.49 | 1 | 0.4 | 150 |
| 28 | 4.75 | 1.25 | 3.80 | 2.49 | 1 | 0.3 | 300 |
| 29 | 4.75 | 2.00 | 4.33 | 3.08 | 1 | 0.1 | 225 |
| 30 | 5 | 0.50 | 2.69 | 1.73 | 1 | 0.1 | 75 |
| 31 | 5 | 0.50 | 2.69 | 1.73 | 1 | 0.3 | 225 |
| 32 | 5 | 0.80 | 3.34 | 2.11 | 1 | 0.4 | 300 |
| 33 | 5 | 1.00 | 3.67 | 2.33 | 1 | 0.5 | 225 |
| 34 | 5 | 1.25 | 3.99 | 2.59 | 1 | 0.2 | 150 |
| 35 | 5 | 2.00 | 4.56 | 3.22 | 1 | 0.5 | 75 |
| 36 | 5 | 2.00 | 4.56 | 3.22 | 1 | 0.3 | 375 |

Experimental Results and Discussions

The produced cups from this experimental plan are measured for four qualities: average diameter deviation from the targeted diameter, average thickness deviation from the targeted thickness, cup surface roughness, and amount of material pile-up. The amount of material pile-up is measured based on the observations that the accumulated formed material pile-up during the ballizing operation is sheared out at the end of the process, causing the cup's material loss. The weight difference between the produced cup weight and the original preformed cup weight equals the amount of cup material loss, which is considered a pile-up size indicator.

Three measures assess the produced cup quality and the pile-up formation severity index. The latter is defined by the weight loss after the cup forming obtained by Eq (7). The quality measures are mainly about the diametral quality, the thickness quality, and the surface quality. The diametral quality measure is the cup diametral deviation from the theoretically targeted cup outer diameter, 62 [mm], which is measured by the average cup diameter deviation percentage obtained by Eq (8). The thickness quality measure is the cup thickness deviation from the theoretically targeted cup wall thickness, 1 [mm], which is measured by the average cup thickness deviation percentage obtained by Eq (9). The surface quality is measured using average roughness Ra along with the cup height. All mentioned quality measures quantify the quality of the produced cup based on the least is the better.

$$\mathbf{W}_{loss} = \frac{\left(\boldsymbol{W_{blank} - W_{cup}}\right)}{\boldsymbol{W_{blank}}} \mathbf{x\ 100\%} \tag{7}$$

$$\boldsymbol{D_{dev}} = \frac{\left(\boldsymbol{D_{av} - D_f}\right)}{\boldsymbol{D_f}} \mathbf{x\ 100\%} \tag{8}$$

$$\boldsymbol{t_{dev}} = \frac{\boldsymbol{t_{av} - C_4}}{\boldsymbol{C_4}} \mathbf{x\ 100\%} \tag{9}$$

The produced cups of the mentioned planned experiments are shown in Figure 3, and the measured quantities are listed in Table 5. The 2nd order response surfaces of the measurements are obtained using MATLAB linear modeling fitting tools. The obtained second-order polynomial fitting for each quality measure relates the four input variables and their interconnection to that measured quality. The coefficients of these polynomials and their root mean square fitting error RMSE are listed in Table 6.

**Table 5:** Measurements of the experimental tests

| Test No. | $W_{loss}$ % | $D_{dev}$ % | $t_{dev}$ % | Ra [□m] |
|---|---|---|---|---|
| | Eq. (2) | Eq. (3) | Eq. (4) | $Ra$ |
| **1** | 20.13394 | 0.75 | -3 | 5.490 |
| **2** | 12.90146 | 2.581 | 102.5 | 5.473 |
| **3** | 14.74118 | 3.726 | 99 | 3.250 |
| **4** | 10.47022 | 4.065 | 126 | 4.050 |
| **5** | 9.984235 | 4.169 | 128 | 3.963 |
| **6** | 10.42983 | 4.137 | 100 | 6.487 |
| **7** | 8.893695 | 5.081 | 161.5 | 3.510 |
| **8** | 13.31058 | 3.234 | 96.5 | 4.137 |
| **9** | 10.40898 | 3.984 | 102.5 | 4.813 |
| **10** | 8.158851 | 4.129 | 115.5 | 4.427 |
| **11** | 10.17837 | 4.702 | 133.5 | 5.223 |
| **12** | 8.48458 | 4.782 | 159 | 5.663 |
| **13** | 9.767951 | 4.742 | 151 | 6.420 |
| **14** | 8.564058 | 5.258 | 158 | 3.450 |
| **15** | 16.54441 | 1.798 | 61 | 5.810 |
| **16** | 17.10727 | 1.218 | 42 | 5.410 |
| **17** | 14.89753 | 3.226 | 107.5 | 5.920 |

| | | | | |
|---|---|---|---|---|
| **18** | 12.54576 | 4.242 | 109 | 5.277 |
| **19** | 6.974502 | 4.718 | 141.5 | 4.980 |
| **20** | 22.08831 | 0.476 | 6.5 | 6.037 |
| **21** | 15.27146 | 1.911 | 86.5 | 7.617 |
| **22** | 13.56464 | 2.532 | 69.5 | 7.677 |
| **23** | 14.86495 | 3.565 | 106 | 8.183 |
| **24** | 10.31127 | 4.032 | 142 | 5.830 |
| **25** | 7.713255 | 5.04 | 150 | 4.807 |
| **26** | 7.568631 | 4.815 | 165.5 | 6.653 |
| **27** | 13.80308 | 3.524 | 86.5 | 6.980 |
| **28** | 9.308022 | 3.379 | 96.5 | 4.090 |
| **29** | 16.24995 | 1.685 | 57 | 5.827 |
| **30** | 21.24272 | 1.194 | -7.5 | 3.113 |
| **31** | 17.2988 | 1.444 | 29 | 8.410 |
| **32** | 14.75811 | 2.702 | 68.5 | 6.557 |
| **33** | 13.30276 | 3.532 | 81 | 6.973 |
| **34** | 18.89878 | 1.806 | 47.5 | 9.780 |
| **35** | 11.27412 | 4.54 | 133 | 5.463 |
| **36** | 7.899571 | 4.323 | 117.5 | 3.760 |

**Table 6: Coefficients of the 2nd Order Response surface for the measured qualities.**

| | **$W_{loss}$ [g]** | **$D_{dev}$ %** | **$t_{dev}$ %** | **Ra [□m]** |
|---|---|---|---|---|
| $C_1$ | 15.979 | 1.1323 | -171.96 | -10.866 |
| $m$ | -44.588 | 9.1599 | 720.59 | 19.735 |
| $f$ | -107.46 | -9.8706 | 1046.3 | 68.49 |
| $N$ | 0.061438 | -0.02973 | -1.094 | 0.029158 |
| $C_1*m$ | -2.0416 | -0.32171 | 21.762 | 2.8946 |
| $C_1*f$ | 5.5885 | -0.61543 | -47.765 | -3.7696 |
| $C_1*N$ | 7.8114 | -3.3493 | -161.55 | -1.3509 |
| $m*f$ | 14.428 | 2.0805 | -67.515 | -21.578 |
| $m*N$ | 13.32 | 11.159 | 79.385 | 5.2008 |
| $f*N$ | 61.795 | -16.19 | -1175.3 | 21.841 |
| $C_1^2$ | -0.02191 | 0.008789 | 0.32644 | -0.0087445 |
| $m^2$ | -0.01672 | -0.00247 | -0.31246 | -0.0050461 |
| $f^2$ | -0.05399 | 0.003484 | -0.07177 | 0.050712 |
| $N^2$ | 0.000127 | -9.43E-06 | 3.08E-05 | -3.00E-06 |
| | | | | |
| **RMSE** | 0.365 | 0.0457 | 7.08 | 0.232 |

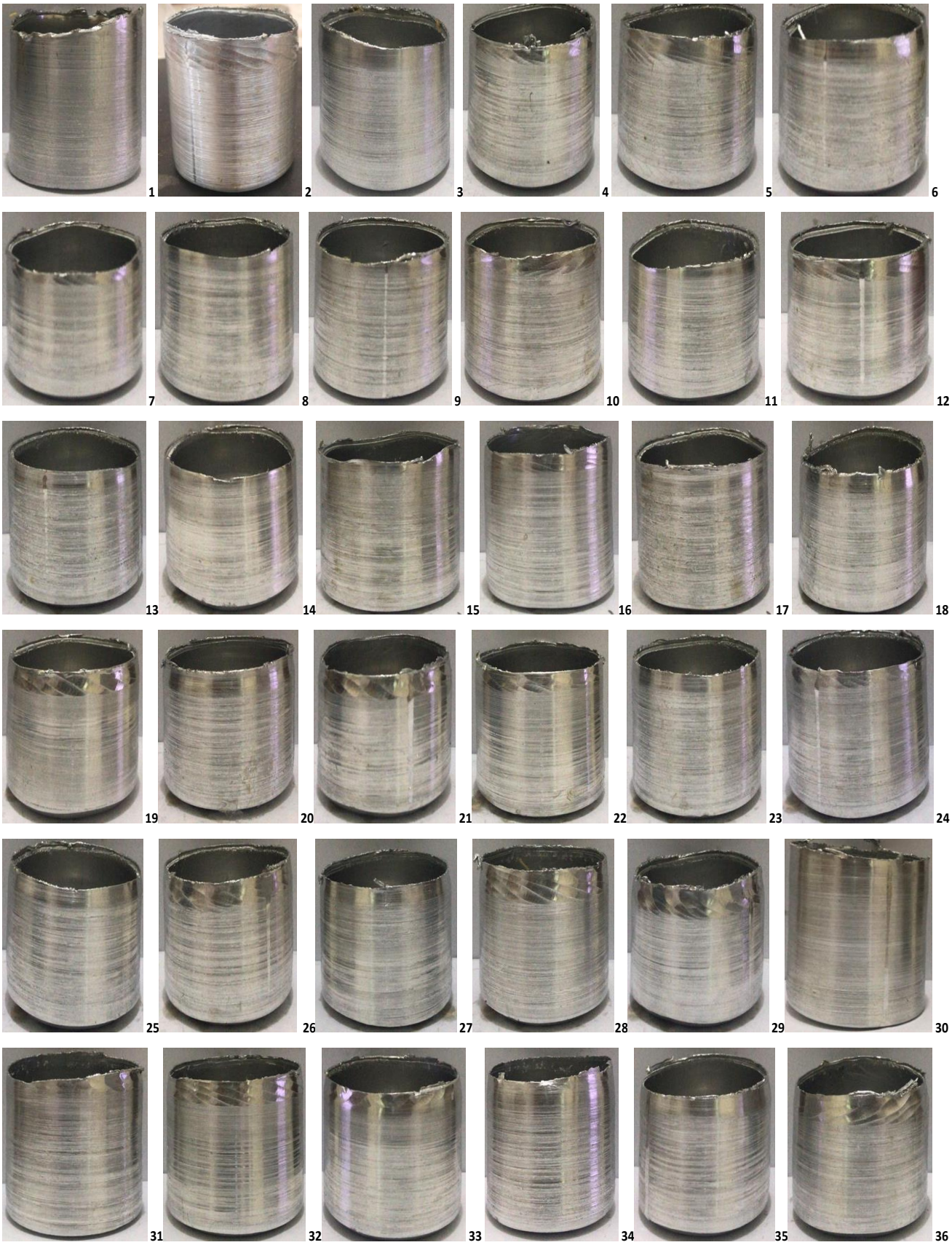


**Figure 3** The produced cups out of the DOE plane

Effect of process parameters on the accumulated material pile up.

As shown in Figure **4**, based on the predicted correlations with all parameters set at their mean values, the material pile-up significantly increases with the first ball clearance ($C_1$). This increase in the pile-up implies that high values of $C_1$ will increase the accumulated left material in the front of the last ball. The correlation also shows that the pile-up has its minimum value with balls arranged in linear profile and increases elsewhere at mean values of the rest of the parameters, as shown in Figure **4.** This observation implies that the evenly distributed thickness reduction helps in reducing the material pile-up. At the conditions with all parameters set at their mean values, the optimum axial feed, ***f***, producing minimum pile up is 0.3 mm/rev, as shown in Figure **4.** It is well observed that the higher the mandrel speed, the lower the pile-up with all investigated parameters set to their mean levels.

The 3D plot for the response surface of the material loss percentage, shown in Figure 4(b), is obtained at the optimum axial feed (f=0.3 mm/rev) and optimum mandrel speed (N=300 rpm), obtained from the correlation. This setup shows an optimum grading index at m= 1.4 for minimum material loss at small first ball clearance $C_1$. However, it shows an optimum grading index at m= 1.0 for minimum material loss at high first ball clearance $C_1$. Generally, the minimum pile-up can be achieved with the first ball clearance set at the minimum tested value C1=4.0 mm and the balls profile index set at m=1.4.

Effect of process parameters on average diameter deviation percentage.

The average cup diameter deviation percentage obtained by Eq (8) is the diametral quality measure in the current work. It reflects the cup diametral deviation from the theoretically targeted cup outer diameter, 62 [mm]. It can be seen from Figure **5**, based on the predicted correlations with all parameters set at their mean values; the correlations show that the average diameter deviation is slightly affected with the increase of the first ball clearance. ($C_1$). However, the average diameter deviation has its maximum value with balls arranged in linear profile and decreases anywhere else. In addition, at mean values of the rest of the parameters, the axial feed, f, gradually increases on average diameter deviation up to 0.4 mm/rev, then it slightly decreases.

Furthermore, with mean values for the rest of the parameters, the average diameter deviation slightly decreases with the decrease of the mandrel rotational speed ***N***. The 3D plot shows that the conditions that reduce the pile-up will worsen the average diameter deviation and vice versa. This observation implies that the proper working conditions depend mainly on the objectives of the spinning process. The manufacturer may be forced to lose material in a pile-up to gain a high-quality cup. Generally, the minimum average diameter deviation percentage can be achieved with the first ball clearance set at the minimum tested value C1=4.0 mm and the balls profile index set at m=0.5.

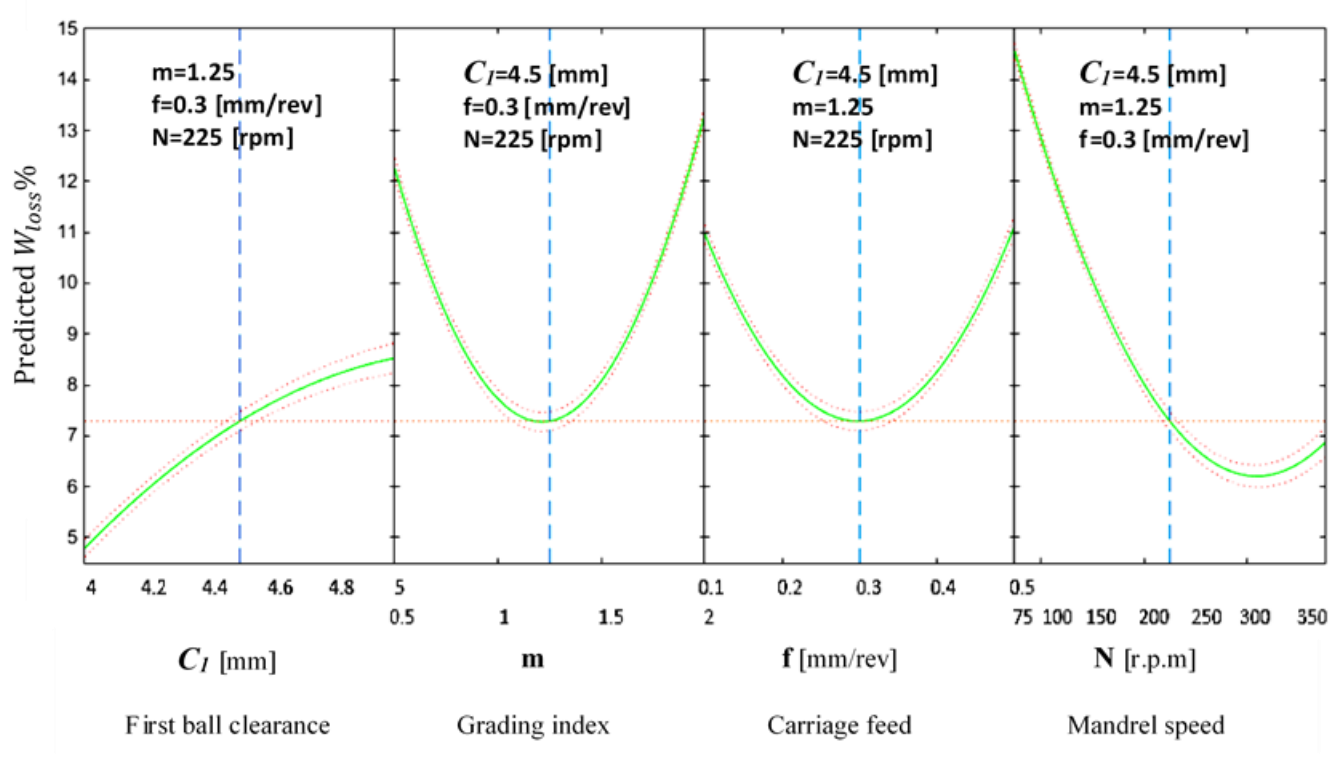


(a) Sliced Plot.

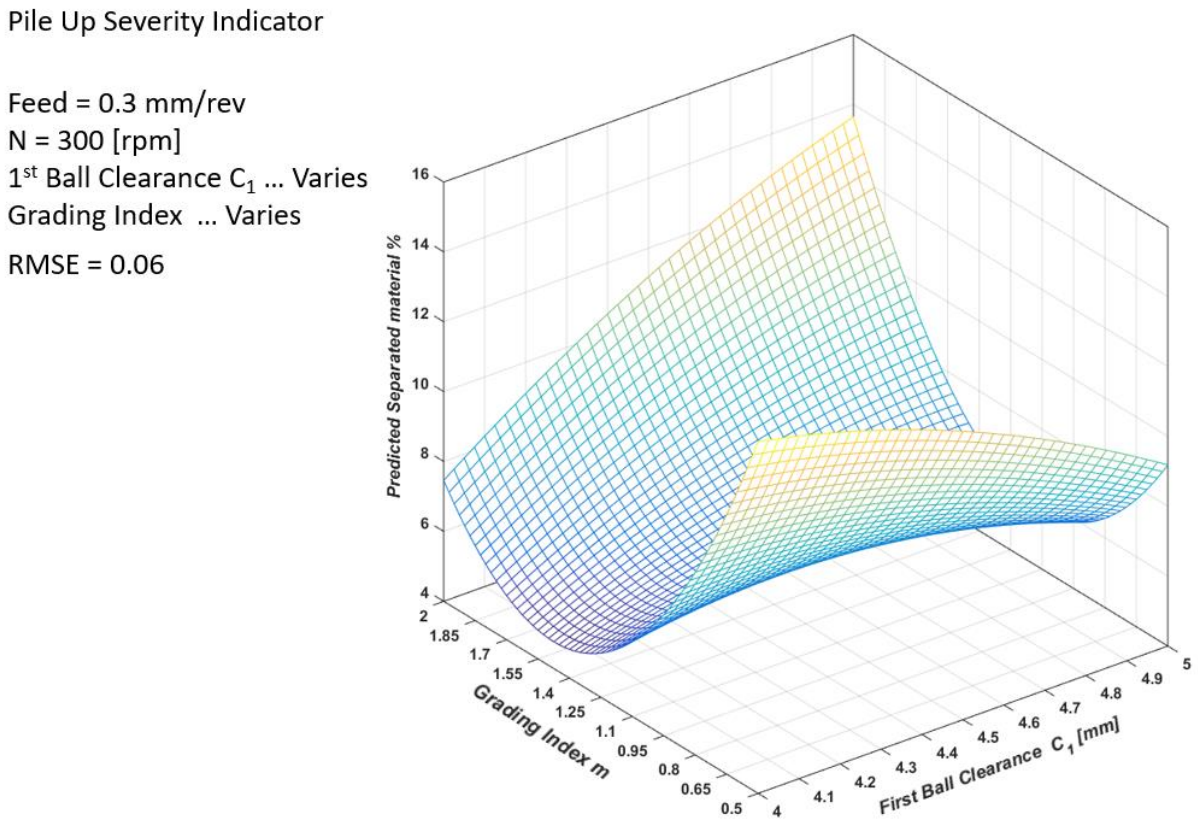


(b) 3D plot.

Figure4: Response surface of the separated material percentage. (a) Sliced Plot. (b) 3D plot.

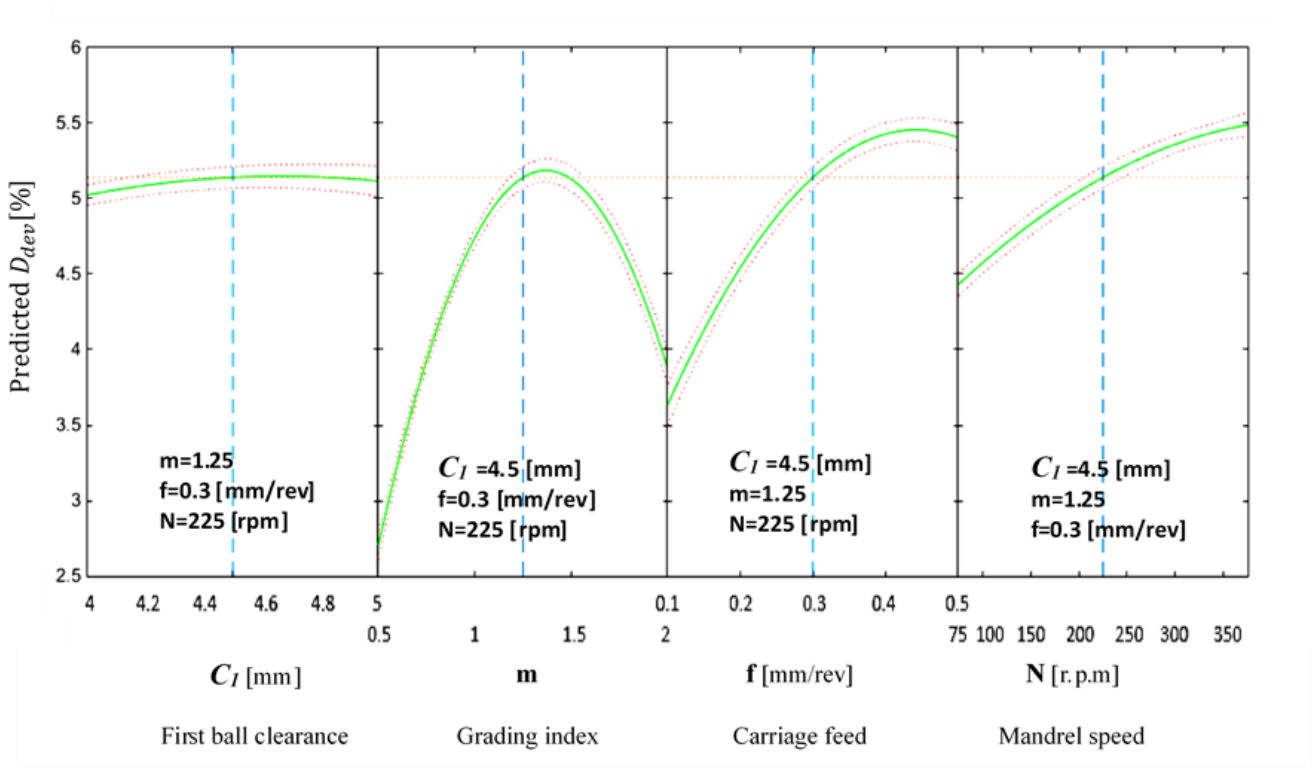


(a) Sliced Plot.

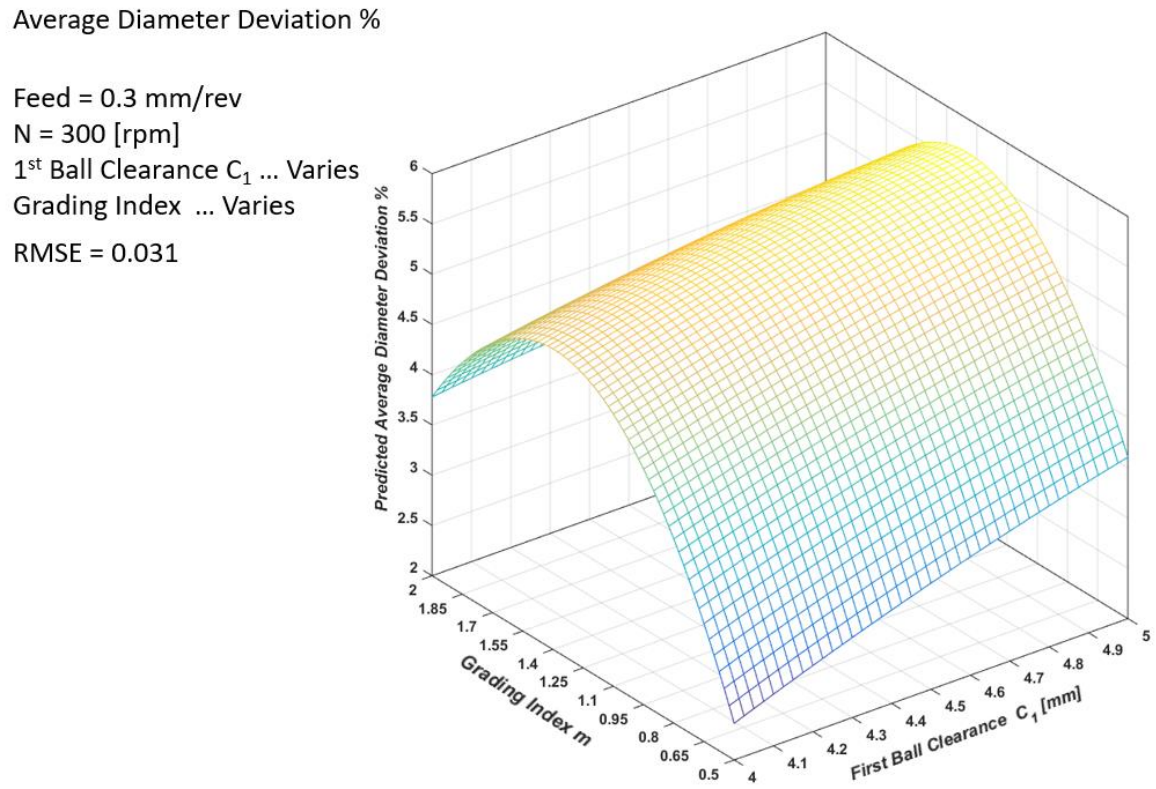


(b) 3D plot.

Figure5: Response surface of the Average Diameter Deviation Percentage. (a) Sliced Plot. (b) 3D plot.

Effect of process parameters on average thickness deviation percentage.

The average cup thickness deviation percentage, obtained by Eq (9), is the thickness quality measure in the current work. It reflects the cup thickness deviation from the theoretically targeted cup wall thickness, 1 [mm]. As shown in Figure **6-a**, based on the predicted correlations with all parameters set at their mean values, the correlations show that the average thickness deviation slightly increases with the distance between the first ball and the mandrel ($C_1$). The correlation also shows that at mean values of the rest of the parameters, the thickness average deviation has its maximum value with balls arranged in slightly concave profile and decrease anywhere else. In addition, at mean values of the rest of the parameters, the axial feed, ***f***, show significant effects on the average thickness deviation. When the average thickness deviation increases, the axial feed increase up to 0.3 mm/rev, then it slightly decreases with the increase of the axial feed. Furthermore, with mean values for the rest of the parameters, the average thickness deviation decreases with the increase of the mandrel rotational speed.

The 3D plot, Figure 6-b, shows that the conditions that reduce the pile-up formation will worsen the average thickness deviation and vice versa. This observation implies that the proper working conditions depend mainly on the objectives of the spinning process. The manufacturer may be forced to lose material in a pile-up to gain a cup with high-quality thickness. Generally, the minimum average thickness deviation percentage can be achieved with the first ball clearance set at the minimum tested value C1=4.0 mm and the balls profile index set at m=0.5.

Effect of process parameters on the average roughness $R_a$.

The surface quality is measured using average roughness Ra along with the cup height in the current work. As shown in Figure **7-a**, based on the predicted correlations with all parameters set at its mean values, the correlations show that the $R_a$ average significantly increases with the increase of the first ball clearance ($C_1$). The correlation also shows that at mean values of the rest of the parameters, the Ra average has its maximum value with balls arranged in linear profile and decreases anywhere else. In addition, at mean values of the rest of the parameters, the Ra average slightly has its minimum value at axial feed, ***f***, of 0.25 mm/rev, while it increases anywhere else. Furthermore, with mean values for the rest of the parameters, the Ra average decreases with the mandrel rotational speed ***N***.

The 3D plot, Figure 7-b, shows that the conditions that reduce the pile-up formation will worsen the average surface roughness and vice versa. This observation implies that the proper working conditions depend mainly on the objectives of the spinning process. The manufacturer may be forced to lose material in a pile-up to gain a cup with a high surface finish. Generally, the minimum average roughness can be achieved with the first ball clearance set at the minimum tested value C1=4.0 mm and the balls profile index set at m=0.5.

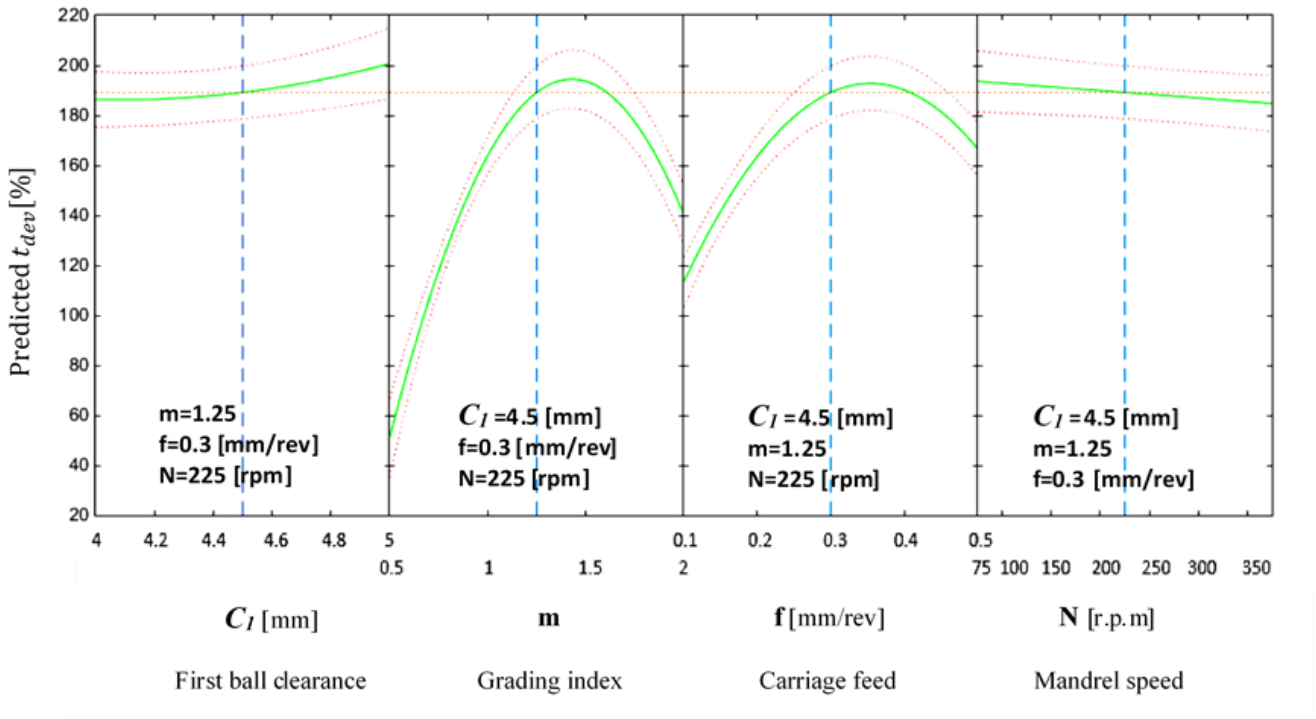


(a) Sliced Plot.

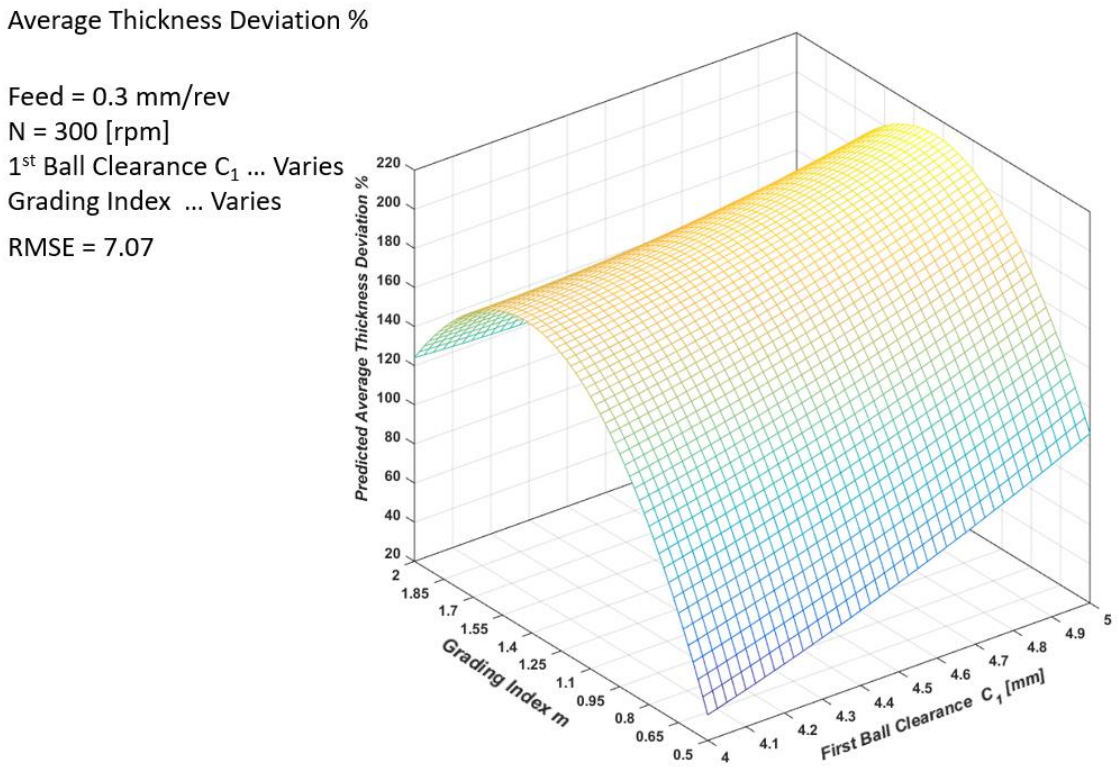


(b) 3D plot.

Figure 6: Response surface of the Average Diameter Deviation Percentage. (a) Sliced Plot. (b) 3D plot.

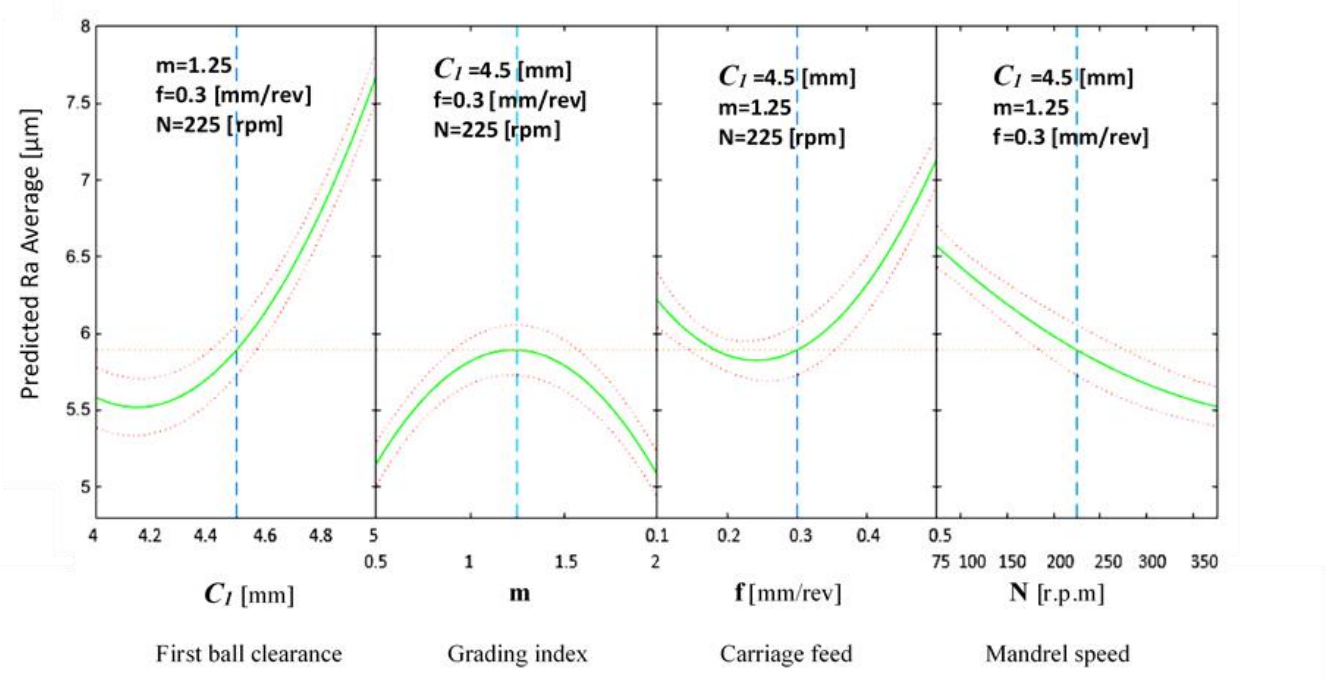


(a) Sliced Plot.

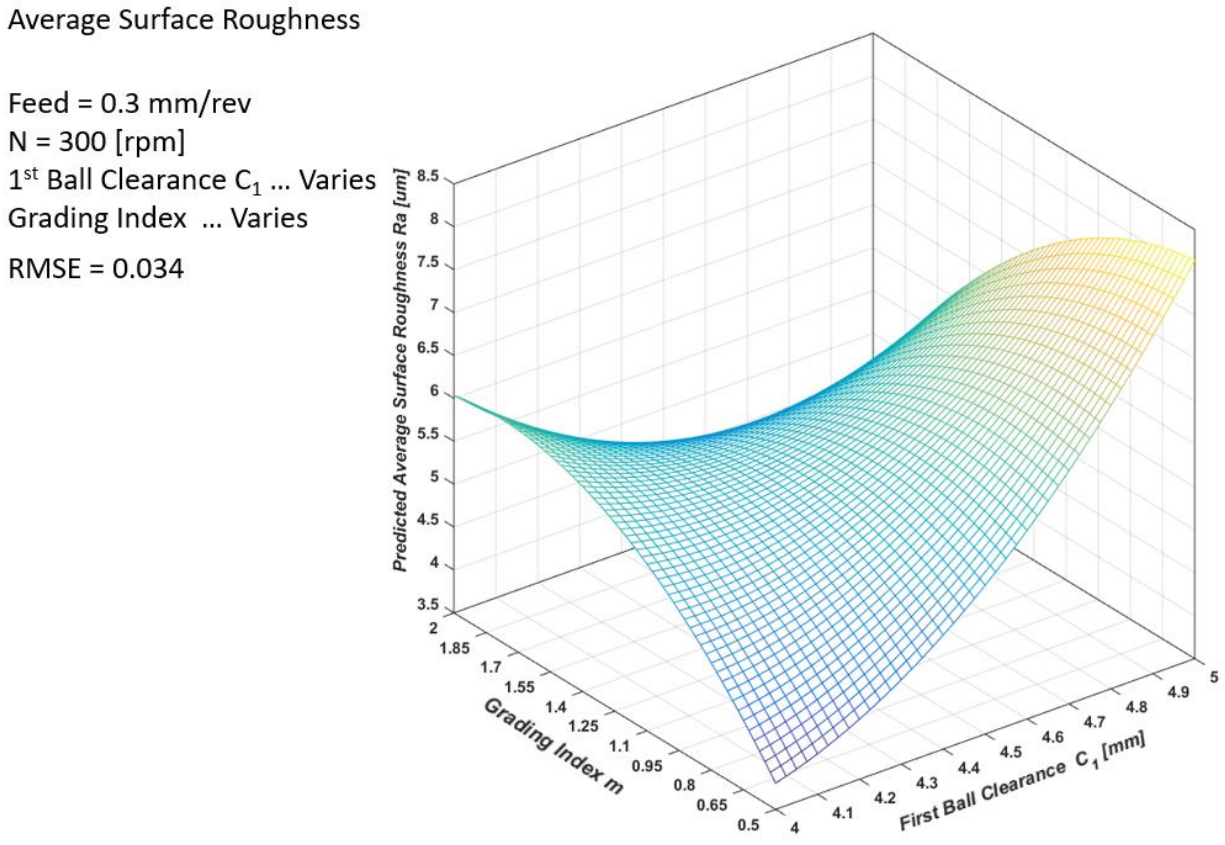


(b) 3D plot.

Figure 7: Response surface of the Average Diameter Deviation Percentage. (a) Sliced Plot. (b) 3D plot.

## 5. Conclusions

The current work presents a new technique in tube spinning using a functionally graded ballizing arrangement. From the experimental work and the preceded surface response analysis, the following conclusions can be obtained:

(1) The new design has shown the potential to significantly overcome the pile-up formation in front of the forming balls at certain balls arrangement.

(2) The current work presents a new approach to assessing the amount of pile-up formation by measuring the material loss percentage after the spinning operation.

(3) The conditions that reduce the pile-up formation will worsen the average diameter deviation percentage, thickness deviation, and surface roughness.

(4) The minimum pile-up can be achieved with the first ball clearance set at the minimum tested value C1=4.0 mm and the balls grading profile index set at m=1.4.

(5) The minimum average diameter deviation percentage, the minimum average thickness deviation, and the minimum average surface roughness can be achieved with the first ball clearance set at the minimum tested value C1=4.0 mm and the balls grading profile index set at m=0.5.

## References


1. Long, Hui, and Seth Hamilton. “Simulation of effects of material deformation on thickness variation in conventional spinning.” In 9th International Conference on Technology of Plasticity, ICTP 2008, pp. 735-740. Hanrimwon Publishing Co., 2008. (DOI:N/A)
2. Shuyong, Jiang, and Ren Zhengyi. “Analysis of mechanics in ball spinning of thin-walled tube.” Chinese Journal of Mechanical Engineering 21, no. 1 (2008): 25-30. (DOI:10.3901/CJME.2008.01.025)
3. Kalpakjian, S., and S. Rajagopal. “Spinning of tubes: a review.” Journal of applied metalworking 2, no. 3 (1982): 211-223. (DOI:10.1007/BF02834039)
4. Rotarescu, M. I. “A theoretical analysis of tube spinning using balls.” Journal of materials processing technology 54, no. 1-4 (1995): 224-229. (DOI:10.1016/0924-0136(94)01772-7)
5. Kim, Naksoo, Honglae Kim, and Kai Jin. “Minimizing the axial force and the material build-up in the tube flow forming process.” International Journal of precision engineering and manufacturing 14, no. 2 (2013): 259-266. (DOI:10.1007/s12541-013-0036-8)
6. Bhatt, Ravi J., and Harit K. Raval. “In situ investigations on forces and power consumption during flow forming process.” Journal of Mechanical Science and Technology 32, no. 3 (2018): 1307-1315. (DOI:10.1007/s12206-018-0235-4
7. Bhatt, Ravi J., and Harit K. Raval. “Investigation on flow forming process using Taguchi-based grey relational analysis (GRA) through experiments and finite element analysis (FEA).” Journal of the Brazilian Society of Mechanical Sciences and Engineering 40, no. 11 (2018): 531. (DOI:10.1007/s40430-018-1456-2
8. Wiens, Eugen, and Werner Homberg. “Internal Flow-Turning–extended manufacturing possibilities in tailored tube production.” In MATEC Web of Conferences, vol. 190, p. 11002. EDP Sciences, 2018. (DOI:10.1051/matecconf/201819011002
9. Wang, Chengyong, Jin Wu, Jinhong Chen, Zhiwei Xiang, and Xiaotao Sheng. “Stability research on spinning of ultra-thin-wall aluminum alloy tube.” SN Applied Sciences 2 (2020): 1-10. (DOI:10.1007/s42452-020-2752-x
10. Zhang, Guang-Liang, Shi-Hong Zhang, Bing Li, and Hai-Qu Zhang. “Analysis on folding defects of inner grooved copper tubes during ball spin forming.” Journal of materials processing technology 184, no. 1-3 (2007): 393-400. (DOI:10.1016/j.jmatprotec.2006.12.016
11. Jiang, Shuyong, Zhengyi Ren, Kemin Xue, and Chunfeng Li. “Application of BPANN for prediction of backward ball spinning of thin-walled tubular part with longitudinal inner ribs.” Journal of materials processing technology 196, no. 1-3 (2008): 190-196. (DOI:10.1016/j.jmatprotec.2007.05.034
12. Jiang, Shuyong, Zhengyi Ren, Chunfeng Li, and Kemin Xue. “Role of ball size in backward ball spinning of thin-walled tubular part with longitudinal inner ribs.” Journal of materials processing technology 209, no. 4 (2009): 2167-2174. (DOI:10.1016/j.jmatprotec.2008.05.006
13. Ahmed, Khaled IE. “A new ball set for tube spinning of thin-walled tubular parts with lon-gitudinal inner ribs.” J Eng Sci 39, no. 1 (2011): 15-32. DOI: 10.21608/jesaun.2011.119713

14. Li, Yong Hua, Tao Fan, and Ning Zhang. “Research on Ball Spinning Forming of Superalloy Inconel 718 Thin-Walled Tube.” In Advanced Materials Research, vol. 189, pp. 2742-2745. Trans Tech Publications Ltd, 2011. (DOI:10.4028/www.scientific.net/AMR.189-193.2742

15. Jiang, Shu-yong, Yan-qiu Zhang, Ya-nan Zhao, T. A. N. G. Ming, and Chun-feng Li. “Finite element simulation of ball spinning of NiTi shape memory alloy tube based on variable temperature field.” Transactions of Nonferrous Metals Society of China 23, no. 3 (2013): 781-787. (DOI:10.1016/S1003-6326(13)62529-7

16. Kuss, M., and B. Buchmayr. “Damage minimised ball spinning process design.” Journal of Materials Processing Technology 234 (2016): 10-17. (DOI:10.1016/j.jmatprotec.2016.03.007

17. Chunjiang, Zhao, Xiong Jie, Huo Xiaodong, Jiang Lianyun, Liu Jiefeng, and Wang Chen. “The analytical model of ball-spinning force for processing an annular groove on the inner wall of a steel tube.” The International Journal of Advanced Manufacturing Technology 91, no. 9-12 (2017): 4183-4190. (DOI:10.1007/s00170-017-0077-8

18. Abd-Eltwab, Ayman A., S. Z. El-Abden, Khaled IE Ahmed, M. N. El-Sheikh, and Ragab K. Abdel-Magied. “An investigation into forming internally-spline sleeves by ball spinning.” International Journal of Mechanical Sciences 134 (2017): 399-410. (DOI:10.1016/j.ijmecsci.2017.10.033

19. Jiang, Shuyong, Yanqiu Zhang, Yanan Zhao, Xiaoming Zhu, Dong Sun, and Man Wang. “Investigation of interface compatibility during ball spinning of composite tube of copper and aluminum.” The International Journal of Advanced Manufacturing Technology 88, no. 1-4 (2017): 683-690. (DOI:10.1007/s00170-016-8803-1

20. Chunjiang, Zhao, Li Guanghui, Xiong Jie, Jiang Zhengyi, Huang Qingxue, Wang Jianmei, and Cui Hailong. “A quasi-dynamic model for high-speed ball spinning.” The International Journal of Advanced Manufacturing Technology 97, no. 5-8 (2018): 2447-2460. (DOI:10.1007/s00170-018-2126-3

21. Zhao, Chunjiang, Feitao Zhang, Jie Xiong, Zhengyi Jiang, Xiaorong Yang, and Hailong Cui. “Plasticity improvement of ball-spun magnesium alloy tube based on stress triaxiality.” Advances in Materials Science and Engineering 2018 (2018). (DOI:10.1155/2018/1735046

22. Zhao, Chun-jiang, Meng-ying Su, Zheng-yi Jiang, Jiang Lian-Yun, Xiaorong Yang, and Hai-long Cui. “Three-directional contact force model for the ball spinning of a thin-walled tube.” Proceedings of the Institution of Mechanical Engineers, Part E: Journal of Process Mechanical Engineering 233, no. 3 (2019): 500-507. (DOI:10.1177/0954408918769431

23. Davidson, M. Joseph, K. Balasubramanian, and G. R. N. Tagore. “Experimental investigation on flow-forming of AA6061 alloy—a Taguchi approach.” journal of materials processing technology 200, no. 1-3 (2008): 283-287. (DOI:10.1016/j.jmatprotec.2007.09.026

24. Razani, N. A., A. Jalali Aghchai, and B. Mollaei Dariani. “Experimental study on flow forming process of AISI 321 steel tube using the Taguchi method.” Proceedings of the Institution of Mechanical Engineers, Part B: Journal of Engineering Manufacture 225, no. 11 (2011): 2024-2031. (DOI:10.1177%2F0954405411398195

25. Srinivasulu, M., M. Komaraiah, and CS Krishna Prasada Rao. “Prediction of the surface roughness of AA6082 flow-formed tubes by design of experiments.” Journal of Mechanical Science and Technology 27, no. 6 (2013): 1835-1842. (DOI:10.1007/s12206-013-0434-y

26. Abedini, Amin, Payam Rahimlou, Taghi Asiabi, Samrand Rash Ahmadi, and Taher Azdast. “Effect of flow forming on mechanical properties of high-density polyethylene pipes.” Journal of Manufacturing Processes 19 (2015): 155-162. (DOI:10.1016/j.jmapro.2015.06.014

27. De, Tarak Nath, Bikramjit Podder, Nirmal Baran Hui, and Chandan Mondal. “Experimental study and analysis of surface roughness of the flow formed H30 alloy tubes.” Materials Today: Proceedings (2020). (DOI:10.1016/j.matpr.2020.09.647

28. Wen, Xue, Jianping Tan, and Xinhe Li. “Research on the drum suppression method for long-distance reverse thinning spinning of the ultra-thin-walled cylinder.” The International Journal of Advanced Manufacturing Technology (2020): 1-18. (DOI:10.1007/s00170-020-05084-5)

29. Khodadadi, M., K. Khalili, and A. Ashrafi. “Studying the Effective Parameters on Teeth Height in Internal Gear Flowforming Process.” International Journal of Engineering 33, no. 12 (2020): 2563-2571. (DOI:10.5829/ije.2020.33.12c.18)

30. Karmoker, J.R.; Hasan, I.; Ahmed, N.; Saifuddin, M.; Reza, M.S. (2019). “Development and Optimization of Acyclovir Loaded Mucoadhesive Microspheres by Box -Behnken Design”. Dhaka University Journal of Pharmaceutical Sciences. 18 (1): 1–12. doi:10.3329/dujps.v18i1.41421.

31. K. T. Fang, D. K. J. Lin, P. Winker and Y. Zhang, “Uniform Design: Theory and Application,” Technometrics, Vols. 42, 2000, no. 3, pp. 237-248. (DOI: 10.1080/00401706.2000.10486045)

32. Z.-z. Liu, W. Li and M. Yang, “Two General Extension Algorithms of Latin Hypercube Sampling,” Mathematical Problen in Engineering, pp. vol. 2015, Article ID 450492, 9 pages, 2015. http://doi.org/10.1155/2015/450492.